Journal of Alloys and Compounds 500 (2010) 252–258

Contents lists available at ScienceDirect

Journal of Alloys and Compounds

journal homepage: www.elsevier.com/locate/jallcom

Photocatalytic activity of nanostructured ZnO films prepared by two different methods for the photoinitiated decolorization of malachite green

Nina Kaneva [a], Irina Stambolova [b], Vladimir Blaskov [b], Yanko Dimitriev [c], Sasho Vassilev [d], Ceco Dushkin [a,*]

[a] Laboratory of Nanoparticle Science and Technology, Department of General and Inorganic Chemistry, Faculty of Chemistry, University of Sofia, 1 James Bourchier Blvd., 1164 Sofia, Bulgaria
[b] Instutute of General and Inorganic Chemistry, BAS, Acad. G. Bonchev St., bl. 11, 1113 Sofia, Bulgaria
[c] University of Chemical Technology and Metallurgy, 8 St. Kliment Ohridski Blvd., 1756 Sofia, Bulgaria
[d] Institute of Electrochemistry and Energy Systems, BAS, Acad. G. Bonchev St., bl. 10, 1113 Sofia, Bulgaria

ARTICLE INFO

Article history:
Received 26 November 2009
Received in revised form 31 March 2010
Accepted 2 April 2010
Available online 10 April 2010

Keywords:
ZnO
Sol–gel
Thin films
Ethylcellulose
Photocatalysis
Malachite green

ABSTRACT

Patterned thin films ZnO are successfully prepared on glass substrates by the sol–gel method using both dip coating and spin coating. Two different procedures are applied for preparation of the films: (i) polymeric one (zinc acetate and ethylcellulose) and (ii) one with complexing agent monoethanolamine (zinc acetate and 2-methoxyethanol). The films of ZnO nanocrystallites with hexagonal crystal structure are characterized by means of scanning electron microscopy, X-ray photoelectron spectroscopy and X-ray diffraction. The films obtained by procedure (i) possess needle-like structure, while the films obtained by procedure (ii) have ganglia on the surface. The as-obtained ZnO films are studied with respect to the photoinitiated bleaching of malachite green (MG) under UV illumination in aqueous solutions. It turns out that the films obtained by procedure (ii) have a better photocatalytic activity than those deposited by procedure (i). It is proven that the films have also some activity in darkness, which is lower than the activities under UV light.

1. Introduction

The zinc oxide represents particular interest from the point of view of its multifunctionality and opportunities of modification and manipulation of various nanostructures. ZnO is a semiconductor with a band gap 3.37 eV, for which reason it is considered as an analogue of the other UV-sensitive members such as GaN, ZnSe, TiO_2. Due to its unique electrical, optical and magnetic properties, its good chemical and thermal stability and its non-toxicity and easy and cheap production, it has found its applications back in the middle of the 20th century [1–4].

The photocatalysis with ZnO represents a perspective research field, because ZnO can be as efficient as TiO_2 in the photocatalytic degradation of some dyes in aqueous solution [5,6]. Therefore, ZnO gains much attention in the degradation and complete mineralization of environmental pollutants [7]. ZnO thin films decompose reactive dyes in their aqueous solutions [5,8], phenol [6], chlorophenol [9], methyl-orange [10], methyl-blue [11], malachite green (MG) [12–14] and other organic environmental pollutants [15–18]. The advantages of using powder catalyst are increased reaction rate due to the increased surface area and simplicity of application. The use of conventional powder catalyst has also disadvantages in stirring during the photocatalytic reaction and in separation of powder after the reaction. The preparation of film catalyst makes it possible to overcome these disadvantages and extend the industrial applications [19]. Furthermore, ZnO is of special interest, because of the possibilities for modification and control of various ZnO-based nanostructures [20–22]. ZnO thin films are prepared by different techniques such as metal organic chemical vapor deposition [23], sol–gel [24,25], thermal evaporation, oxidation and anodizing [26–28]. The sol–gel process and utilization of dip-coating technique is one of the versatile strategies to prepare thin films of particles. Recent research demonstrates the possibilities for utilization of ZnO thin films, prepared by the sol–gel method [29,30], which is very attractive low-cost and versatile method for deposition of homogeneous thin films with desired thickness and nanostructure.

As the efficiency of photocatalytic processes is attributed to the presence of more active centers, it is important to find the way for preparation of films with porous structure. To solve this problem, various non-ionic and polymer-type surfactants such as polyethylene glycol (PEG) [31] and polyvinyl alcohol (PVA) [32] have been widely applied in the sol–gel process. To the best of our knowledge, the studies concerning preparation of photocatalyti-

* Corresponding author. Tel.: +359 2 8161 387; fax: +359 2 962 5438.
E-mail address: nhtd@wmail.chem.uni-sofia.bg (C. Dushkin).

0925-8388/$ – see front matter © 2010 Elsevier B.V. All rights reserved.
doi:10.1016/j.jallcom.2010.04.020

cally active ZnO–polymer nanocomposite films are very scarce [33]. Chakrabarti et al. have investigated the degradation of polyvinyl chloride films in aqueous medium using (PVC)–ZnO composite films [33].

There are not data in the available literature about the preparation of polymer composite ZnO films using ethylcellulose as a modifier. The ethylcellulose is a polymer with abundant R–OH and R–O–R bonds in its molecular structure. The lone electron pairs in the ether–oxygen atoms and hydroxyl–oxygen atoms can interact with the vacant orbitals of metal ions. So it enhances the homogeneity of metal ions in the precursor and thus prevents the aggregation of the particles during heating. In addition, the ethylcellulose is a long chain, soluble and non-ionic substance, which can induce the crystallization of ZnO during the coating process. For the above reasons we choose ethylcellulose as a structure-directing agent added into the starting solutions in order to obtain porous films, which is the key parameter for a good photocatalytic activity. We call this manner of film preparation as procedure (i).

The classical sol–gel method using complexing agent monoethanolamine (MEA) [12] is also applied for the deposition of ZnO films in order to compare them with the films obtained by polymeric formulation. We will refer to this preparation of thin films as procedure (ii).

The aim of this paper is to compare the structural and photocatalytic properties of porous ZnO sol–gel films, prepared by procedures (i) and (ii) with respect to the decolorization of malachite green in water.

2. Experimental

2.1. Preparation of ZnO films

Materials: Zinc acetate dihydrate $Zn(CH_3COO)_2{\cdot}2H_2O$ (>99.5%), 2-methoxyethanol (>99.5%) and monoethanolamine (>99%) were from Fluka. Malachite green (MG) oxalate was from Croma-G mbH & Co. The glass slides (ca. 76 mm × 26 mm), used for substrates of the ZnO films, were from ISO-LAB (Germany). The soda-lime microscope glasses were cleaned with a chromerge solution (H_2SO_4/Cr_2O_3), then with a mixture of hydrochloric and nitric acid and finally with ethanol and acetone successively.

Polymeric sol–gel method, procedure (i): zinc acetate and ethylcellulose as polymer additive were dissolved into ethanol–water mixture of (3:1) to obtain 0.4 M solution (sol A). The solution of ethylcellulose in ethanol was prepared by 24 h stirring (sol B) and then added to sol A under vigorous stirring for 3 h (under standard conditions without controlling of the humidity in air). The as-prepared mixture was used for deposition (sol C). The ethylcellulose in sol C was 40 wt% relative to the zinc concentration in sol solution. The films were deposited on cleaned substrates by spin coating at 1500 rpm for 30 s, Every coating was dried at 120 and 240 °C for 15 min and finally was annealed at 350 °C for 1 h. This deposition-treatment cycle was repeated five times. The scheme of experimental procedure (i) is presented in Fig. 1a.

Sol–gel with complexing agent, procedure (ii): The scheme of procedure (ii) is shown in Fig. 1b. Zinc acetate dihydrate (10 g), 2-methoxyethanol (20 ml) and monoethanolamine (3.2 ml) [12] are mixed together in a round-bottomed flask and stirred at room temperature for 15 min. The obtained clear solution was heated up at 60 °C upon magnetic stirring for 1 h and let aging overnight. The resultant solution was clear and homogenous to serve as the coating substance for film preparation. No visible changes were observed in the solution upon standing at room temperature for at least 2 months.

The deposition of ZnO films consisted of dip-coating, drying and sintering of the material. Dipping a glass substrate in the precursor solution and withdrawing it at rates of 0.9 cm/min at room temperature prepared the gel films. It was found that higher withdrawal rates resulted in films of lower quality. The films were dried at 80 °C for 30 min after each successive coating. The final gel films were preheated at 350 °C for 15 min and then sintered at 500 °C for 60 min in order to obtain the ZnO films for photocatalytic tests. The mass of ZnO film deposited on glass for five coatings was 5.2 mg (±8%). The film area was about 14.5 cm^2 on each side of the glass plate.

2.2. Characterization of ZnO films

The obtained ZnO thin films were first imaged by a scanning electron microscope (SEM) JSM-5510 (JEOL), operated at 10 kV of acceleration voltage. The investigated samples were coated with gold by JFC-1200 fine coater (JEOL) before the observation.

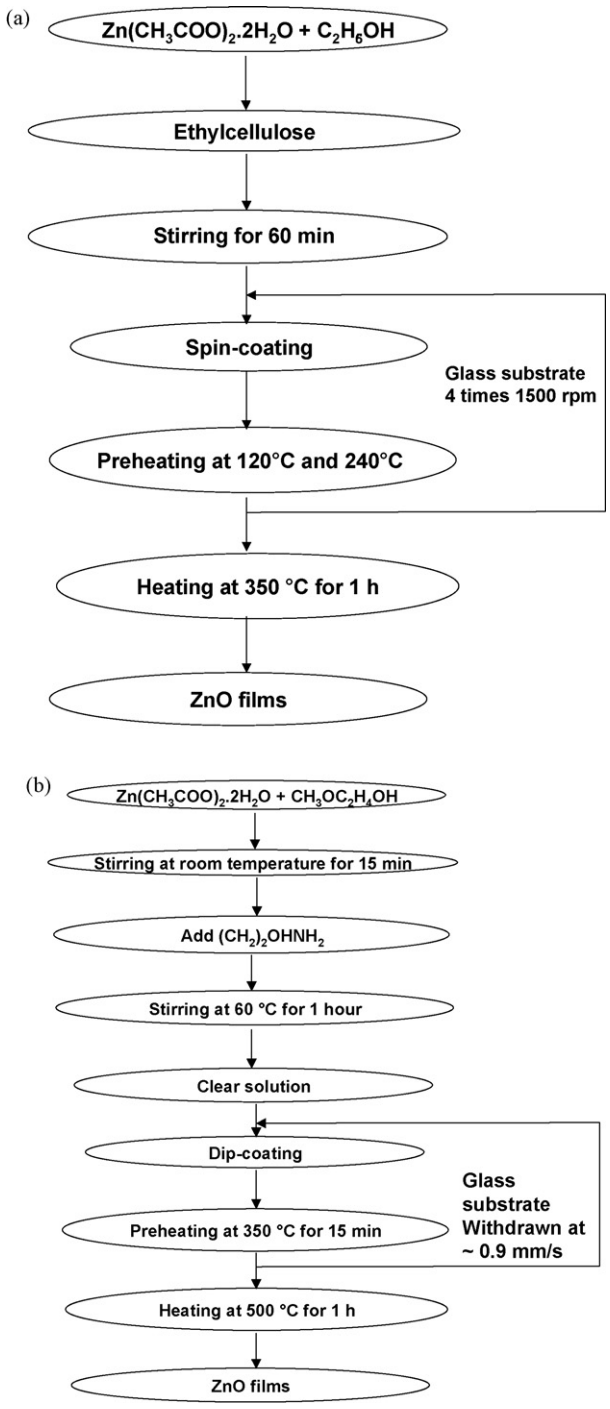

Fig. 1. Scheme of experimental procedures: (a) procedure (i) and (b) procedure (ii).

The X-Ray diffraction (XRD) spectra of ZnO thin films were recorded at room temperature on a powder diffractometer (Siemens D500 with a source of CuKα radiation) within 2θ range of 10–80° at a step of 0.05° of 2θ and counting time 2 s/step.

The surface composition and electronic properties of the zinc oxide films were investigated by X-ray photoelectron spectroscopy (XPS). The measurements were performed in a VG ESCALAB II electron spectrometer using a source of AlKα radiation with energy of 1486.6 eV. The binding energies (BE) were determined with an accuracy of ±0.1 eV utilizing the C 1s line at 285.0 eV (from an adventitious carbon) as a reference. The composition and chemical surrounding of the films were investigated on the basis of the areas and binding energies of C 1s, O 1s, Zn 3p photoelectron peaks and Scofield's photoionization cross-sections.

The photocatalytic activities of ZnO films were assessed by the photoinitiated bleaching of 5-ppm MG in aqueous solution. The photocatalytic reaction was conducted in a cylindrical glass vessel of volume of 150 ml, equipped with a magnetic

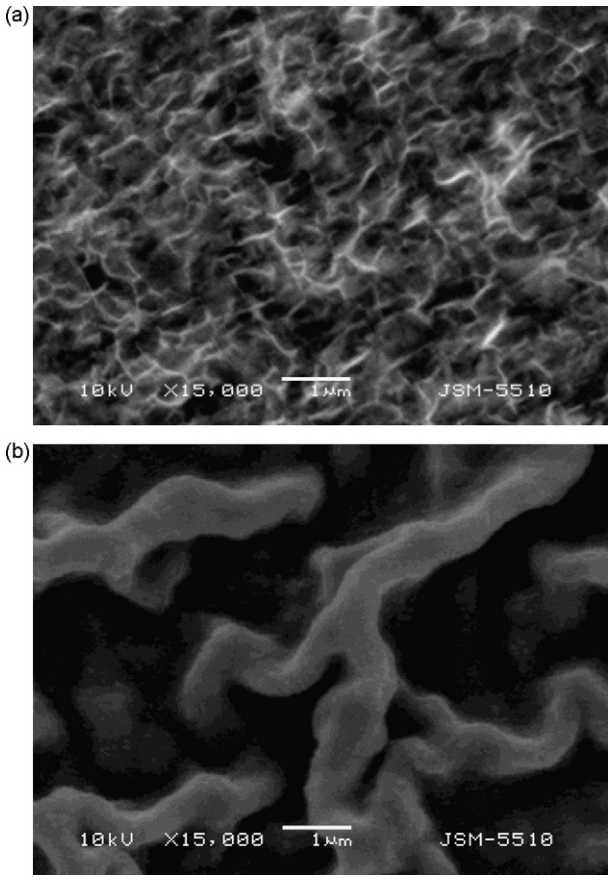

Fig. 2. SEM images of ZnO film prepared by procedure (i) (a) and procedure (ii) (b).

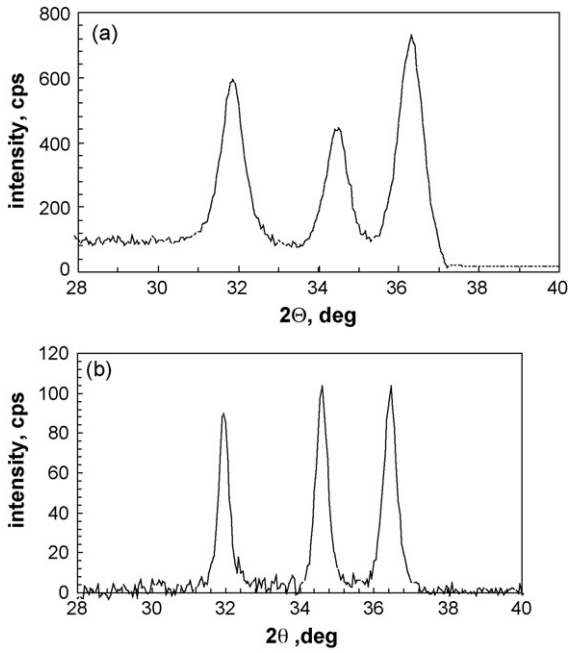

Fig. 3. XRD spectra of ZnO films annealed for 1 h at 350 °C (procedure (i)) (a) and (b) annealed for 1 h at 500 °C (procedure (ii)). The crystallite sizes are about 12.4 and 30 nm in both cases.

stirrer (rotating speed controlled by stroboscope) and UV-lamp (Sylvania BLB, 18 W, maximum emission at 315–400 nm). The light power density at the sample position was 0.66 mW/cm^2 as measured with Research Radiometer (Ealing Electro-optics, Inc.). The time decay of MG concentration during the bleaching process was monitored by UV–vis absorbance spectroscopy after aliquot sampling at regular time intervals. Control experiments without UV light (the reaction system kept in dark) were also performed. All photocatalytic tests were performed at a constant stirring rate (500 rpm) at room temperature (25 °C). The sample was equilibrated in the dark for about 5 min before irradiation commenced. The optical absorbance spectra were measured by spectrophotometer Jenway 6400 in the wavelength range from 400 to 800 nm. The actual dye concentration $C(t)$ in the solution was calculated from the measured absorbance by the linear relationship derived in Appendix A.

3. Results and discussion

3.1. Structure characterization

The SEM image of the sample obtained by procedure (i) is shown in Fig. 2a. It can be seen from the image that the addition of 40 wt% ethylcellulose to the sol results in films with a rough surface and needle-like structure. It is established that the films obtained from solutions containing more than 40% polymer have poor quality and adhesion to the substrate, which affects also their photocatalytic performance.

The ethylcellulose probably promotes the formation of a porous netlike structure with many ramifications. Kim and Francis [34] have obtained titania coatings using titanium ethoxide and hydroxypropylcellulose, which posses a similar porous structure. Previous experimental results of our group, concerning the deposition of titania–ethylcellulose composite films, have also shown similar type of morphology. According to the thermogravimetric analysis between 130 and 330 °C, made by Zhou et al. [35] the weight loss is attributed to the oxidation and carbonization of cellulose. Obviously the processes of ethylcellulose decomposition, accompanied by the evolution of gas and heat generated during the combustion, lead to the appearance of porous structure.

The SEM image of ZnO films obtained by procedure (ii) is shown in Fig. 2b. Different ganglia-like hills are seen of typical width 1 μm and length from 5 to 15 μm. The ganglia are located on the surface of film being of typical height about 2.5–3 μm. They are reproducible irrespective on the conditions of film deposition and we can see them in always different films. A ganglion comprises nanograins of ZnO similar to those in the continuous film in-between.

The X-ray diffraction studies reveal that all films obtained by procedure (i) are polycrystalline without a preferred orientation and the spectral peaks (1 0 0), (0 0 2) and (1 0 1) correspond to hexagonal wurtzite structure (Fig. 3a). The mean crystallite size, estimated by the Sherrer′s formula for the polymeric-derived films, is 12.4 nm.

The phase structure of glass-supported ZnO thin films made by procedure (ii) confirms the formation of hexagonal ZnO (peaks at $2\theta = 31.9°$, 34.6° and 36.4°) with average size of the crystallites of about 30 nm (Fig. 3b).

The surface composition and chemical state of the ZnO films are investigated by XPS. In Fig. 4 are shown the Zn 2p and O 1s peaks of the films before the photocatalytic tests (curves 1) and after tests (curves 2).

The Zn $2p_{3/2}$ peak for the oxide film is located at 1021.8 eV, typical for zinc in ZnO (Fig. 4a, curve 1). In the O 1s spectrum of a fresh sample predominates the O^{2-} component at 530.0 eV as seen from the spectrum deconvoluted by Lorentzian–Gaussian fitting into three peaks in Fig. 5a. The second component at 530.8 eV is ascribed to O^{2-} in the vicinity of oxygen vacancies formed in the ZnO film according to [34,35] The third peak at ~532.2 eV is due to oxygen bonded in OH^- and $-CO_3$ groups.

After the photocatalytic reaction, the Zn 2p, C 1s and O 1s, photoelectron peaks of sample (ii) become wider compared to those before photocatalytic tests (Fig. 4a and b, curves 2). Likely, the reason for this is the formation of several phases with different charging during the photoemission. The Zn $2p_{3/2}$ peak in Fig. 4c is fitted with two components, attributed to zinc atoms coordinated

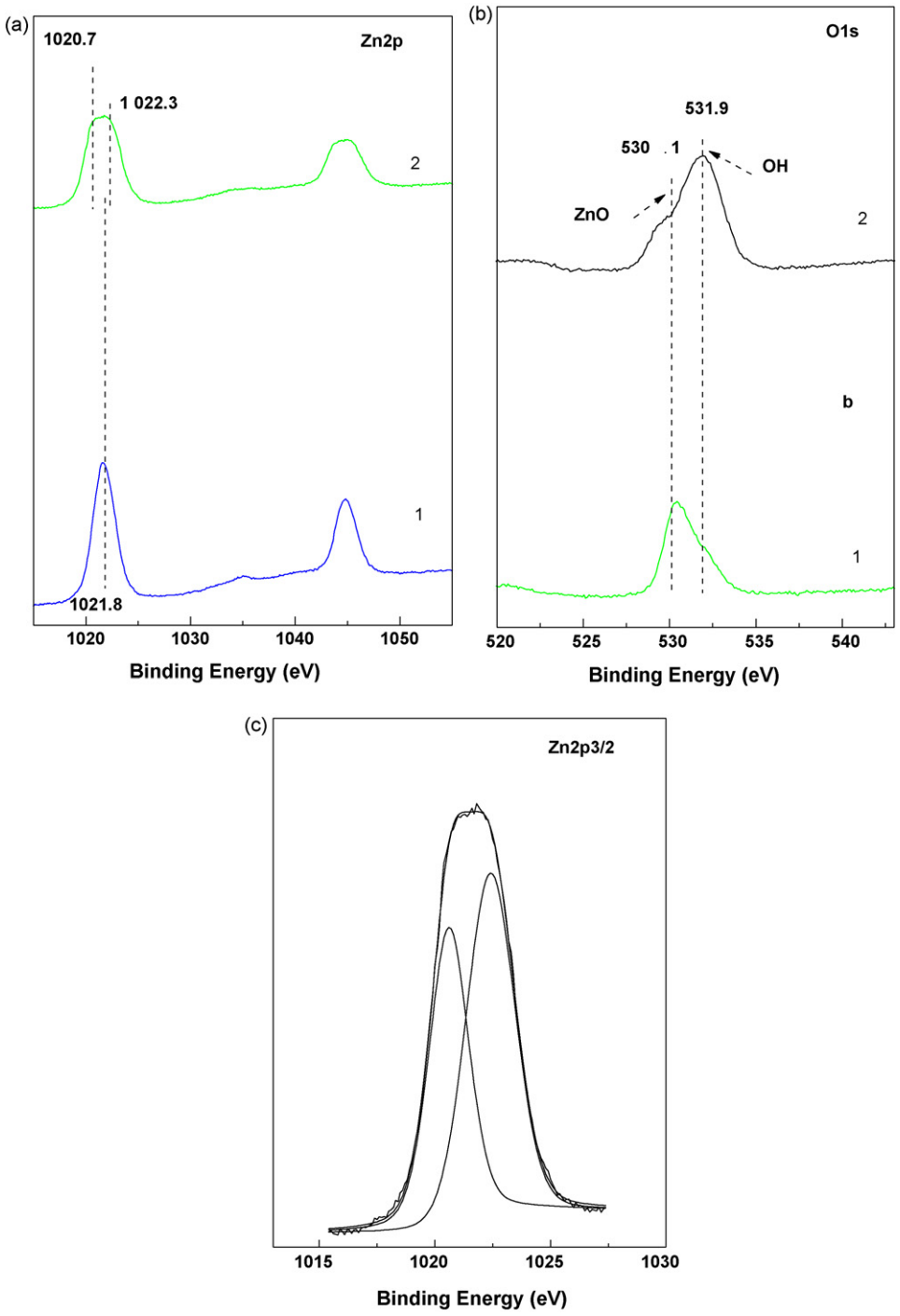

Fig. 4. XPS spectra of Zn 2p line (a) and O 1s (b) of ZnO films obtained by procedure (i). Curves 1 are for sample before photocatalysis; curves 2 – after that. (c) Zn $2p_{3/2}$ peak of ZnO layers after UV irradiation (enlarged from curve 2 in (a)). The thin lines show deconvolution of the spectrum into two peaks.

in ZnO (1020.7 eV) and zinc atoms bonded to OH^- and $-CO_3$ groups (1022.3 eV), respectively.

A similar shift in the position of Zn 2p and O 1s peaks in XPS spectra after photocatalytic tests are registered also for the films, obtained by method (i). The O ls peak of a sample after catalysis is deconvoluted into three components with increasing binding energy. They are attributed to O^{2-} ions in ZnO lattice, O^{2-} ions in oxygen-deficient regions within the matrix of ZnO and oxygen in bonded $-CO_3$ or OH^- groups, respectively (Fig. 5b).

3.2. Characterization of the photocatalytic activity

Three sets of experiments are performed in order to prove the photocatalytic activity of ZnO films with respect to MG degradation. First, experiments on the exposure of MG to ZnO films under UV illumination. Second, experiments performed at the same other conditions, but without UV illumination. Third, experiments to expose MG aqueous solutions to UV light without the presence of ZnO in the solution (the photolysis condition). In this case no visi-

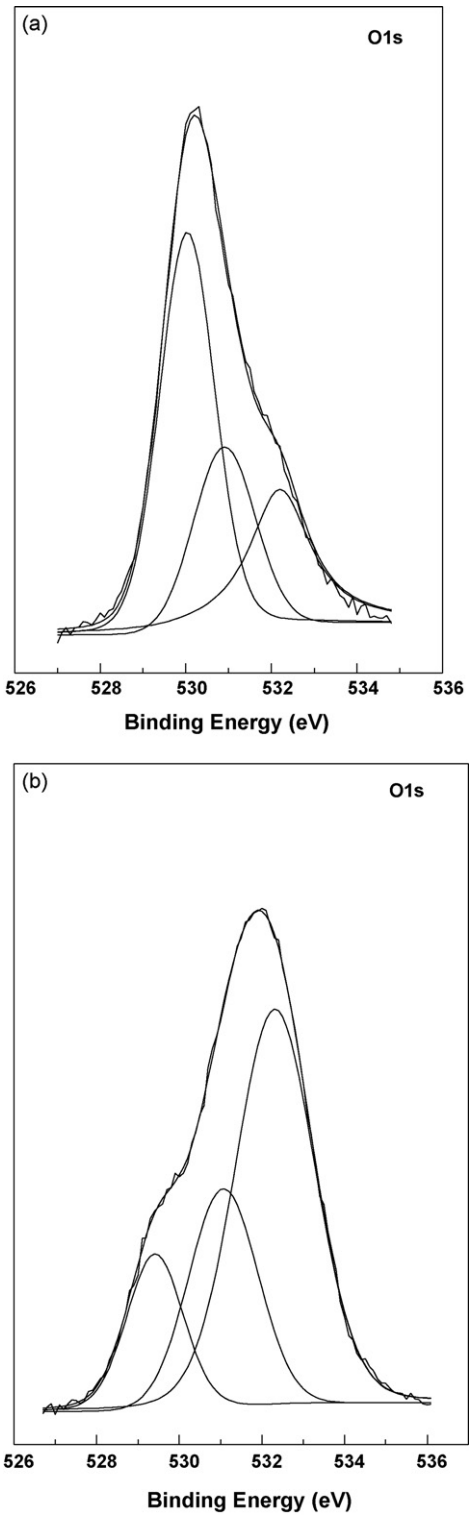

Fig. 5. XPS spectra of O 1s of ZnO films obtained by procedure (ii) for a fresh sample (a) and after UV irradiation in MG solution (b). The thin lines are deconvolution spectra with three single peaks (see the text).

ble decomposition of MG is observed implying on the fact that the ZnO is only responsible for the decrease of dye concentration.

Now let us consider the decolorization of MG by ZnO films under UV illumination (photocatalysis conditions). The results from these experiments are presented in Figs. 6 and 7. Fig. 6 demonstrates the bleaching kinetics of MG aqueous solutions by both kinds of ZnO films exposed and not exposed to UV light illumination. In

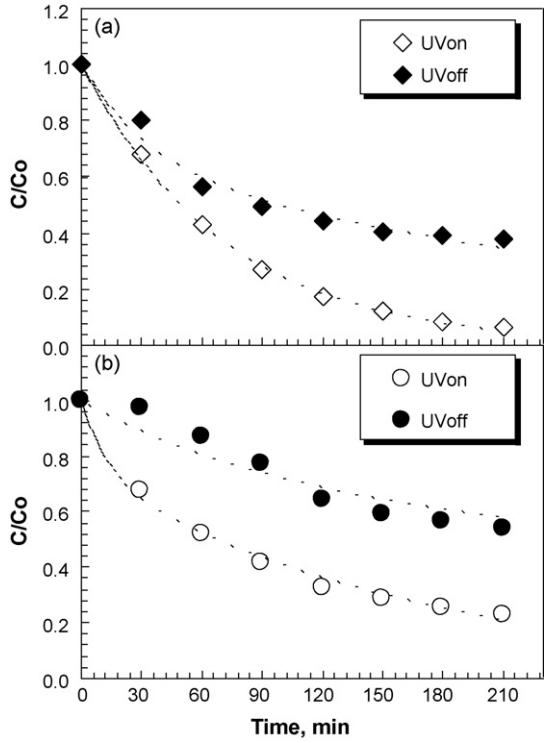

Fig. 6. Decrease of the MG concentration $C(t)$ in aqueous solutions with and without UV light illumination: (a) ZnO films prepared by procedure (ii); and (b) ZnO films by procedure (i). The initial MG concentration C_0 is 5 ppm. The lines are theoretical fits of the data using two-exponential model Eq. (1).

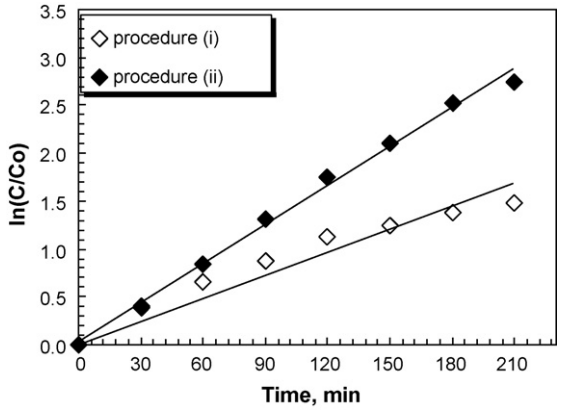

Fig. 7. Decolorization kinetics of MG aqueous solutions by ZnO films with UV light illumination. The photocatalytic process at UV light follows first-order kinetics according to the equation $\ln(C/C_0) = -kt$ (solid lines). Here C_0 is the initial concentration of dye solution, $C(t)$ is the concentration at time t, and k is the rate constant of photocatalysis.

both cases the decolorization kinetics is well described by the two-exponential equation [36]

$$\frac{C(t)}{C_0} = Be^{-k_1 t} - (1 - B)e^{-k_2 t} \quad (1)$$

where $C(t)$ is the actual dye concentration at time t, C_0 is the initial dye concentration, B is a matching constant, k_1 is the rate constant of adsorption of the dye on the film of catalyst and k_2 is the rate constant of dye decomposition. Eq. (1) is derived assuming a two-stage process: initial adsorption of the dye on the photocatalyst surface (fast stage) followed by the dye destruction during the photocatalysis (slow stage).

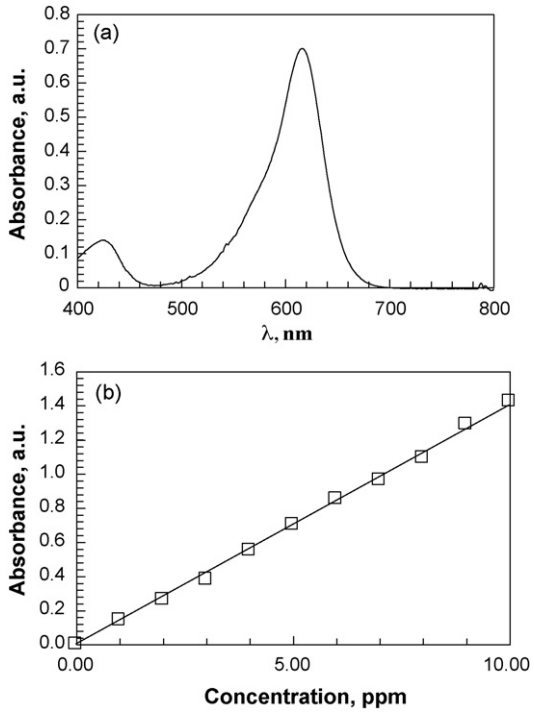

Fig. 8. (a) Absorbance spectrum of MG in a water solution of concentration $C_0 = 5$ ppm and (b) the calibration line of the absorbance maxima at wavelength 615 nm versus the dye concentration. The straight line is data fit by Eq. (A.2).

The thin films, prepared by procedure (ii) and illuminated with UV (rate constant $k_2 = 0.014\,\text{min}^{-1}$), show a better photocatalytic activity than the films obtained by procedure (i) ($k_2 = 0.006\,\text{min}^{-1}$). The results could be explained with the different morphological characteristics of the films: the classical sol–gel method without polymer leads to a more developed surface, than the polymeric method (see Fig. 2). The films prepared by procedure (i) possess very fine crystallites (12.4 nm), but their photocatalytic activity is relatively low. Obviously, the photocatalytic properties are more sensible to the type and area of the film surface, rather than the size of crystallites.

It is interesting also to see the decolorization of MG by ZnO films without UV illumination (Fig. 6). As seen from the figure, the concentration of MG also decreases without UV illumination, but the decomposition of dye is slower in comparison with the respective photocatalytic reactions ($k_2 = 0.003\,\text{min}^{-1}$ for case (ii) and $k_2 = 0.0009\,\text{min}^{-1}$ for case (i)), reaching almost constant value after about 3 h. The decrease of MG concentration in this case is most probably due to the adsorption on the ZnO films (with respective rate constants $k_1 = 0.03\,\text{min}^{-1}$ and $k_1 = 0.001\,\text{min}^{-1}$) or due to a sort of chemical activity of the ZnO even in the darkness. We were not able to measure the net adsorption of MG on ZnO thin films. But we could compare our results with the adsorption of methylene blue on a thin film of TiO_2 (Degussa P25) [36,37]. The characteristic time of the process is about 4 min, which is much smaller than the time constant of the process with thin films of ZnO measured by us, which fact does not support the assumption for prevailing dye adsorption on the film surface during the dark experiments. Moreover, our measurements of the absorbance of thin ZnO films, used in the dye decolorization showed that there is no residual dye deposited on the film within the experimental error (Appendix B).

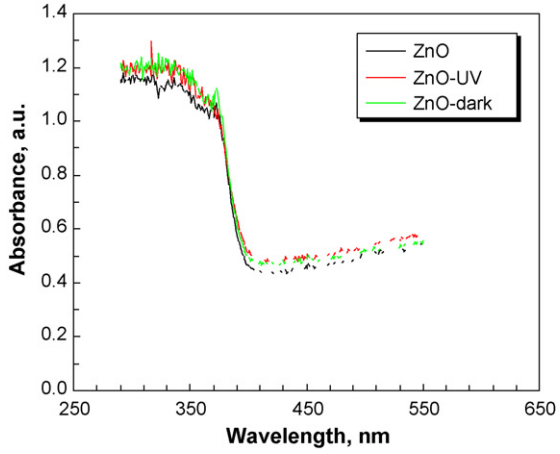

Fig. 9. Comparison of the absorbance spectra of ZnO thin films used in the decolorization of dye malachite green.

The rate constants can also be calculated from the data presented in Fig. 7 assuming pseudo-first-order reaction kinetics for photocatalysis and using the initial slope of the curves. The results for the rate constants are $k = 0.008\,\text{min}^{-1}$ for the films obtained by procedure (i) and $k = 0.0138\,\text{min}^{-1}$ for the films by procedure (ii). These values of k are close to the respective k_2 and corroborate with the degree of MG decomposition in the presence of the ZnO films, obtained by both procedures.

4. Conclusions

ZnO nanosized sol–gel thin films were obtained by two different manners. All films pertain to the hexagonal wurtzite structure without preferred orientation irrespective to the manner of film preparation. The addition of ethylcellulose as structure-directing agent in procedure (i) affects the formation of nanocrystalline structure by suppression of sintering and leads to a porous needle-like structure with crystallite size about 12–15 nm. Sol–gel procedure (ii) using MEA and 2-methoxyethanol leads to the formation of other type film morphology which consist of ganglia-like hills. The crystalline sizes are about 30 nm. XPS spectra of the films reveal that after photocatalytic tests the O 1s peaks become wide and asymmetric and could be divided into two components. The photocatalytic activities of the films obtained by polymeric sol–gel method are lower than those of the films obtained by sol–gel method. The results obtained show that the films morphology has more significant influence on the properties than the size of the crystallites. The ZnO thin films prepared by us are promising and efficient catalyst for photocatalytic degradation of malachite green.

Acknowledgements

This work is financially supported by project TK-X-1702/07 of the Bulgarian Ministry of Education and Science. CD is also thankful to COST D-43 Action of the European Community and project UNION DO02-82 of the National Science Fund of Bulgaria.

Appendix A. Calibration of the absorbance versus dye concentration

The malachite green dye exhibits two maxima of absorbance at 405 and 620 nm, respectively. For the purpose of measurements, we utilize the second maximum since it is much better pronounced thus allowing a better sensitivity of detection (Fig. 8a). Fig. 8b plots the absorbance maximum A at 615 nm versus the dye concentration in the solution C (in ppm). The calibration plot (correlation coefficient 0.998) shows the linear dependence of optical absorbance on the dye concentration expressed as

$$A = 0.14C \quad \text{(A.1)}$$

This equation confirms the validity of the Bouguer–Lambert–Beer low for our system in the form

$$A = \varepsilon LC \quad (A.2)$$

where $L = 1$ cm is the width of glass cuvette and ε is the molar absorption coefficient ($\varepsilon = 0.14\,cm^{-1}\,ppm^{-1}$). This fact is used further to obtain the actual dye concentration in the solution.

Appendix B. Measurement of the thin film absorbance

Fig. 9 compares the absorbance spectra of thin films of ZnO as mentioned in the legend: as-prepared film (ZnO), a thin film used in the UV-decolorization of the dye MG and a thin film used in darkness. As seen from the figure, there is no evidence at 620 nm for the eventual absorbance of dye accumulated on the ZnO film in the course of dye adsorption.

References

[1] H. Mead, Phys. Lett. 18 (1965) 218.
[2] K.S. Kirkpatrick, T.O. Mason, Jpn. J. Appl. Phys. 10 (1971) 736.
[3] B. Balzer, M. Hagemeister, P. Kocher, L.J. Gauckler, J. Am. Ceram. Soc. 87 (2004) 1932.
[4] K. Mukae, Ceram. Bull. 66 (1987) 1329.
[5] C.A.K. Gouvea, F. Wypych, S.G. Moraes, N. Duran, N. Nagata, P. Peralta-Zamora, Chemosphere 40 (2000) 433.
[6] B. Dindar, S. Icli, J. Photochem. Photobiol. A: Chem. 140 (2001) 263.
[7] M.C. Yeber, J. Rodriguez, J. Freer, N. Duran, H.D. Mansilla, Chemosphere 41 (2000) 1193.
[8] C. Lizama, J. Ferrer, J. Baeza, H.D. Mansilla, Catal. Today 76 (2002) 235.
[9] S. Lathasree, A.N. Rao, B. Siva-Sankar, B. Sadasivam, K. Rengaraj, J. Mol. Catal. A: Chem. 223 (2004) 101.
[10] C. Wang, X. Wang, Bo-Qing Xu, J. Zhao, B. Mai, Ping'an. Peng, G. Sheng, J. Fu, J. Photochem. Photobiol. A Chem. 168 (2004) 47.
[11] Y. Jang, C. Simer, T. Ohm, Mater. Res. Bull. 41 (2006) 67.
[12] N.V. Kaneva, G.G. Yordanov, C.D. Dushkin, Bull. Mater. Sci., in press.
[13] N.V. Kaneva, G.G. Yordanov, C.D. Dushkin, React. Kinet. Catal. Lett. 98 (2009) 259.
[14] N.V. Kaneva, G.G. Yordanov, C.D. Dushkin, in: E. Balabanova, I. Dragieva (Eds.), Nanosci. Nanotechnol., vol. 9, Marin Drinov Publishing House, Sofia, 2009, pp. 54–57.
[15] L.B. Khalil, W.E. Mourad, M.W. Rophael, Appl. Catal. B: Environ. 17 (1998) 267.
[16] C. Sirtori, P.K. Altvater, A.M. de Freitas, P.G. Peralta-Zamora, J. Hazard. Mater. 129 (2006) 110.
[17] H. Akyol, C. Yatmaz, M. Bayramoglu, Appl. Catal. B Environ. 54 (2004) 19.
[18] N. Daneshvar, D. Salari, A. Khataee, Appl. Catal. B Environ. 162 (2004) 317.
[19] K. Iketani, R.D. Sun, M. Toki, K. Hirota, O. Yamaguchi, Mater. Sci. Eng. B 108 (2004) 187.
[20] M. Andres-Verges, A. Mifsud, C. Serna, Mater. Lett. 8 (1989) 115.
[21] M. Andres-Verges, M. Martinez-Gallego, J. Mater. Sci. 27 (1992) 375.
[22] S. Haile, D. Jonson, G. Wiesemen, H. Bowen, J. Am. Ceram. Soc. 72 (1989) 227.
[23] J.L. Yang, S.J. An, W.I. Park, G.Y. Yi, W. Choi, Adv. Mater. 16 (2004) 1661.
[24] B. Pal, M. Sharon, Mater. Chem. Phys. 76 (2002) 82.
[25] F. Peng, S.H. Chen, L. Zhang, H.J. Huang, Z.Y. Xie, Acta Phys. Chem. Sinica 21 (2005) 944.
[26] O.A. Fouad, A.A. Ismail, Z.I. Zaki, R.M. Mohamed, Appl. Catal. B: Environ. 62 (2006) 144.
[27] Ya.I. Alivov, A.V. Chernykh, M.V. Chukichev, R.Y. Korotkov, Thin Solid Films 473 (2005) 241.
[28] Y. Yamaguchi, M. Yamazaki, S. Yoshihara, T. Shirakashi, J. Electroanal. Chem. 442 (1998) 1.
[29] F. Peng, H. Wang, H. Yu, S. Chen, Mater. Res. Bull. 41 (2006) 2123–2129.
[30] G. Delgado, C.I. Romero, S.A. Hernandez, R. Perez, O. Angel, Solar Energy Mater, Solar Cells 93 (2009) 55.
[31] Zh. Liu, Zh. Jin, W. Lei, J. Qin, Matter. Lett. 59 (2005) 3620.
[32] T. Du, H. Song, O.J. Ilegbusi, Mater. Sci. Eng. B 27 (2007) 414.
[33] S. Chakrabarti, B. Chandhuri, S. Bhattacharjee, P. Das, B.K. Dutta, J. Hazard. Mater. 154 (2008) 230.
[34] Y.-J. Kim, L.F. Francis, J. Mater. Sci. 33 (1998) 4423–4433.
[35] Y. Zhou, En-Y. Ding, Wei-Dong Li, Mater. Lett. 61 (2007) 5050–5052.
[36] M. Kostadinov, C. Dushkin, D. Mladenova, M. Uzunova-Bujnova, L. Petrov, G. Li Puma, submitted for publication.
[37] R.W. Matthews, J. Chem. Soc. Faraday Trans. 85 (1989) 1291.